Published in final edited form as:
J Biol Chem. 2007 November 30; 282(48): 34634–34643. doi:10.1074/jbc.M705301200.

STRUCTURAL AND FUNCTIONAL CHARACTERISATION OF RECOMBINANT MATRILIN-3 A-DOMAIN AND IMPLICATIONS FOR HUMAN GENETIC BONE DISEASES

Maryline Fresquet[1], **Thomas A. Jowitt**[1], **Joni Ylöstalo**[2], **Paul Coffey**[3], **Roger S. Meadows**[1], **Leena Ala-Kokko**[4,5], **David J. Thornton**[1], and **Michael D. Briggs**[1,*]

[1]Wellcome Trust Centre for Cell-Matrix Research, Faculty of Life Sciences, University of Manchester, Manchester, M13 9PT, UK [2]Center Center for Gene Therapy, Tulane University Health Sciences, New Orleans, LA 70123, USA [3]School of Physics & Astronomy, University of Manchester, Manchester, UK [4]Collagen Research Unit, Biocenter Oulu and Department of Medical Biochemistry and Molecular Biology, University of Oulu, FIN-90014 Oulu, Finland [5]Connective Tissue Gene Tests, Allentown, Pennsylvania, USA

Abstract

Mutations in matrilin-3 result in multiple epiphyseal dysplasia (MED), which is characterized by delayed and irregular bone growth and early onset osteoarthritis. The majority of disease-causing mutations are located within the β-sheet of the single A-domain of matrilin-3, suggesting that they disrupt the structure and/or function of this important domain. Indeed, the expression of mutant matrilin-3 results in its intracellular retention within the rER of cells, where it elicits an unfolded protein response.

In order to understand the folding characteristics of the matrilin-3 A-domain we determined its structure using circular dichroism, analytical ultracentrifugation and dual polarization interferometry. This study defined novel structural features of the matrilin-3 A-domain and identified a conformational change induced by the presence or the absence of Zn^{2+}. In the presence of Zn^{2+} the A-domain adopts a more stable 'tighter' conformation. However, after the removal of Zn^{2+} a potential structural rearrangement of the MIDAS motif occurs, which leads to a more 'relaxed' conformation.

Finally, in order to characterize the interactions of the matrilin-3 A-domain we performed binding studies on a BIAcore using type II & IX collagen and COMP. We were able to demonstrate that it binds to type II & IX collagen and COMP in a Zn^{2+}-dependent manner. Furthermore, we have also determined that the matrilin-3 A-domain appears to bind exclusively to the COL3 domain of type IX collagen and that this binding is abolished in the presence of a disease causing mutation in type IX collagen.

Keywords

Multiple epiphyseal dysplasia; matrilin-3; A-domain; conformational change; type IX collagen; cartilage oligomeric matrix protein

[*]**Corresponding author**, Michael D. Briggs, Faculty of Life Sciences, University of Manchester, Michael Smith Building, Oxford Road, Manchester, M13 9PT. Tel. +44 161 275 5642, Fax. +44 161 275 5082, Email: mike.briggs@manchester.ac.uk.

Europe PMC Funders Author Manuscripts

Matrilin-3 is a heteromeric extracellular matrix (ECM) protein (50 kDa) which is primarily expressed in the cartilage growth plate (1,2). Matrilin-3 has a modular structure comprising a von Willebrand factor A (vWFA) domain (A-domain), four epidermal growth factor (EGF)-like domains and a coiled-coil domain, which facilitates oligomerisation (1-4). Mutations in the A-domain of matrilin-3 have been shown to result in some forms of multiple epiphyseal dysplasia (MED), an autosomal dominant skeletal dysplasia characterized by short-limb dwarfism and early onset osteoarthritis (5,6). The majority of *MATN3* mutations that cause MED are missense mutations found within the β-strands and are predicted to affect the folding of the A-domain (6,7). Previous *in vitro* and *in vivo* studies have shown that mutant matrilin-3 protein is retained within the rER of cells and elicits an unfolded protein response (7-9). This essentially renders biochemical and biophysical analysis of the effects of the mutations very difficult since it is not possible to isolate these recombinant mutant proteins under non-denaturing conditions.

MED is genetically heterogeneous and can also result in mutations in the genes encoding cartilage oligomeric matrix protein (COMP) and type IX collagen (*COL9A1, COL9A2* and *COL9A3*) (Reviewed in (10)). COMP is the fifth member of the thrombospondin protein family (11) and is found primarily in cartilage, tendon and ligament (12-15). Like matrilin-3 it is a modular protein and comprises a coiled-coil domain, four type II (EGF-like) repeats, seven type III (TSP3) repeats and a large C-terminal globular domain (CTD) (16). *COMP* mutations are found in both the TSP3 (85%) and CTD (15%) domains of COMP and are either missense mutations or small in-frame deletions or insertions (17,18). Type IX collagen is a heterotrimer of α1(IX) α2(IX) α3(IX) chains and a member of the FACIT (Fibril Associated Collagen with Interrupted Triple helices) group of collagens (19). It consists of three collagenous domains (COL1-3) separated by non-collagenous domains (NC1-NC4) and is closely associated with type II collagen, where it is thought to act as a molecular bridge between type II/XI collagen fibrils and other cartilage matrix proteins (19). The large NC4 domain is derived entirely from the α1(IX) gene (*COL9A1*) and along with the other NC domains has been shown to bind to the CTD of COMP *in vitro* (20,21). Interestingly, type IX collagen gene mutations have a very restricted distribution and all of them are postulated to cause an in-frame deletion from equivalent regions of the COL3 domain in the α1(IX), α2(IX) or α3(IX) chains (Reviewed in (10)). This precise grouping of type IX collagen gene mutations has yet to be fully explained, however it is possible that these deletions may disrupt important interactions with other components of the cartilage ECM either directly, by deleting a binding site within the COL3 domain, or indirectly by changing the orientation of the α1(IX)NC4 domain relative to the type II/XI collagen fibril.

Insight into the conformation of the matrilin-3 A-domain can be provided by striking sequence similarities with the I-domain of α1-integrin (6). The matrilin-3 A-domain, as well as the I-domain, adopts a Rossman fold with 7 α-helices surrounding a central β-sheet comprising 6 β-strands (22). The top face of both domains contain a non-contiguous Metal Ion-Dependent Adhesion Site (MIDAS) (23). Interactions at the MIDAS site of the integrin I-domain have been linked to a ~10Å shift in the position of the α-7 helix and results in a tertiary switch of the domain (22). This change in conformation is not just linked directly to binding of the metal ion, but rather to a cooperative interaction of the cation and ligand to provide the 'outside-in' signaling event. It has been hypothesized that A-domains, which contain a 'perfect' MIDAS motif, might also bind metal ions and undergo a similar 'integrin-like' switch in conformation (24). To date the ability of the A-domain of matrilin-3 to bind to cations and/or undergo a conformational change has not been determined. We therefore investigated if the human matrilin-3 A-domain was capable of binding metal ions and might also undergo a change in conformation similar to that of integrin I-domains. Zn^{2+} and Ca^{2+} ions were selected since they are the most biologically relevant cations. Zn^{2+} has been shown to play important biological roles in cartilage organization (25). In this study we

have demonstrated that recombinant matrilin-3 A-domain can also adopt different conformations through a specific interaction with Zn^{2+}.

The precise function of matrilin-3 is still not fully understood, however, it has previously been described as a potential matrix-adaptor or ECM bridging molecule and is known to interact with a number of cartilage ECM proteins such as COMP and type IX collagen (26,27). A-domains are known to mediate protein-protein interactions (23) and it is therefore possible that the single matrilin-3 A-domain has evolved a selective affinity for different types of cartilage molecules and participates in the assembly of the fibril network in the cartilage ECM (28,29). In this study we tested the ability of the matrilin-3 A-domain alone to bind to type II and type IX collagen in the presence of different cations. Binding assays were also performed in the presence of EDTA to determine if the cation-dependent conformational change in the structure of the A-domain affected its binding properties. We were able to demonstrate that the matrilin-3 A-domain binds with high affinity to full-length type IX collagen in a Zn^{2+}-dependent manner. Furthermore, this binding was abolished when the type IX collagen contained an in-frame deletion previously shown to cause MED (30-32), suggesting that the matrilin-3 A-domain binds to amino acid sequences in the COL3 domain of type IX collagen. These data therefore provide the first insight into why MED mutations might cluster in the COL3 domain of type IX collagen.

EXPERIMENTAL PROCEDURES

Cloning and sequencing of human matrilin-3 A-domain

The matrilin-3 A-domain (contained in exon 2 of *MATN3*) had previously been amplified from genomic DNA by PCR and subcloned into pSecTag (6). This fragment was then subcloned a second time into pCEP4. The forward primer encompassed the first 20 nucleotides (from the ATG start codon) of the Ig γ-chain secretion signal found in pSecTag and included a *Not*I restriction site (primer 5′-gcggccgcatggagacagacacact-3′). The 3′-primer (5′-gcggccgctcacttatcgtcgtcatccttgtaatcacagaaggtttcctggaatct-3′) also contained an engineered *Not*I cleavage site in addition to an in-frame FLAG Tag (DYKDDDDK). PCR products were cloned using TA Cloning method (Invitrogen) and sequenced using M13R and M13 (-20) primers with ABI Prism dye terminator cycle sequencing reagents (PerkinElmer Life Sciences). These sub-clones were digested with the restriction enzyme *Not*I and cloned into the pCEP4 expression vector (Invitrogen). Following transformation into TOP10 cells (Invitrogen) positive clones were obtained which contain the correct nucleotide sequences in the right orientation. A single clone (pCEP4-MATN3WT) was used for all subsequent experiments.

Matrilin-3 A-domain expression and purification

Purified pCEP4-MATN3WT DNA was transfected into 293-EBNA cells (human embryonic kidney cells; Invitrogen) using LipofectAMINE 2000 reagent (Invitrogen). The cells were cultured in Dulbecco's modified Eagle medium containing 10% foetal calf serum and after 24h transfected cells were selected by the addition of Hygromycin B (50 μg/ml). Following cell confluency the medium was replaced with serum free VPRO medium (JRH Biosciences). The cells were incubated in this medium for a further 48h before the conditioned medium was collected and centrifuged at 1000 x g for 4 minutes. The resulting supernatant (400 ml) was affinity purified using the FLAG Tag. Briefly, the conditioned medium was incubated with the anti-FLAG M2 affinity column (Sigma) for 1h at 4°C. Bound proteins were eluted from the beads with FLAG peptide (50 μg/ml) in 20 mM Tris pH7.4, 150 mM NaCl. Fractions (1 ml) were collected and analysed by SDS-PAGE with silver staining. The fractions containing the matrilin-3 A-domain were desalted using PD-10

columns (GE Healthcare) and further purified by anion exchange chromatography on a MiniQ column using the Ettan purifier HPLC system (GE Healthcare).

Cloning of vitreous form of human type IX collagen

The vitreous form of collagen IX was generated using previously constructed full-length α1(IX) cDNA (33) in pVL1392 vector (Pharmingen) as a template for PCR. The 72 nucleotide alternative exon 1 of α1(IX) was generated 5′ to COL3 domain in three consecutive PCR reactions using the previous reaction as a template for the next reaction. JYeye1 (5′-CTG TTG GGG CTC TGC TTG TGC GCG GCT CAA AGA GGT CCC CCG GGT GAG CAG-3′) and JYeyeR (5′-AGG AAT ACC ACG GCC TGG AAA TCC AC-3′) primers were used in the first reaction, JYeye2 (5′-GCG CGG GAC CGC GGG GCC CTG GGG CTG CTG CTG TTG GGG CTC TGC TTG TGC-3′) and JYeyeR in the second, and JYeye3 (5′-AGT CAT TGC GGC CGC ATG GCC TGG ACT GCG CGG GAC CGC GGG GCC CTG-3′) and JYeyeR in the third. JYeye3 primer contained an engineered *Not*I cleavage site. Final PCR product was ligated to pGEM-T-Easy vector (Promega) and sequenced (Big Dye Terminator v3.0, ABI Prism 3100 Genetic Analyzer, Applied Biosystems). The resulting plasmid and full-length α1(IX) cDNA in pVL1392 vector were digested with *Not*I and *Sbf*I and the generated alternative exon 1 containing piece was ligated to the digested α1(IX) cDNA in pVL1392 vector. The resulting construct was sequenced.

Cloning of MED mutant form of human type IX collagen

To generate the MED mutant form (containing a 12 amino acid deletion in COL3 domain) of α3(IX) chain, previously constructed full-length α3(IX) cDNA in pVL1392 vector (33) was digested with *Xba*I and ligated to pGEM-3Zf(+) vector (Promega). The plasmid was cut with *Not*I and *Stu*I to remove exon 3. mRNA was isolated from a MED mutant patient and reverse transcriptase was used to generate the cDNA containing the mutation. The cDNA was used in PCR with FIC (5′-GGC GGC CGC CGG GGC GCA GAG G-3′) and MH40 (5′-GCT CAC TCC TGC CTC TCC GG-3′) primers. PCR product was ligated to Sure Clone vector followed by cutting with *Not*I and *Stu*I. The resulting piece was ligated to previously cut 9A3 cDNA in pGEM-3Zf(+) vector. The resulting 9A3 MED construct was cut from plasmid with *Xba*I and ligated to *Xba*I cut pVL1392 and sequenced.

Expression and purification of human type IX collagen constructs

The cDNAs constructed above were co-transfected into *Spodoptera frugiperda* (Sf9, Invitrogen) insect cells with a modified *Autographa californica* nuclear polyhedrosis virus using the BaculoGold™ Transfection Kit (Pharmingen). Sf9 cells were cultured in TNM-FH medium (Sigma) supplemented with 10% fetal bovine serum (FBS, Atlanta Biologicals) at 27°C and were seeded at ~60% confluency in tissue culture plates for the transfection. The viral pools were plaque purified and amplified 3-4 times using monolayer (~70% confluency) cultures.

Trichoplusia ni (High Five, Invitrogen) insect cells were cultured in suspension in Sf-900 II SFM medium (Gibco) with or without 5% FBS at 27°C. Prior to the infection, the insect cells were seeded at 1-1.5 × 10^6 cells/ml for expression. The cells were co-infected with three viruses containing cDNAs for the various α1(IX), α2(IX) and α3(IX) chains and a double promoter virus 4PHαβ for the α and β subunits of human prolyl 4-hydroxylase cDNAs (34), with a multiplicity of infection (MOI) of 2 for each virus. Ascorbate (80 μg/ml) was added to the culture medium daily.

After 72 h of infection, the High Five cells were harvested by centrifugation at 1,000 x g for 30 min at 4°C, and the medium was further clarified at 10,000 x g for 30 min. Collagen IX

molecules were precipitated from the culture medium by adding solid ammonium sulfate to 26% saturation and placing the mixture on ice while stirring for 1h. The precipitate was collected by centrifugation at 10,000 x g for 30 min at 4°C and dissolved in 0.4 M NaCl, 2 M urea, 10 mM EDTA, 0.1 M Tris-HCl, pH 7, buffer at 4°C overnight. The protein solution was clarified by centrifugation at 12,000 x g for 30 min at 4°C and then purified by gel filtration (Superdex™ 200, Amersham Biosciences) in the same buffer. The protein was further purified by cation exchange chromatography (HiTrap™ SP HP or SP FF, Amersham Biosciences) in 50 mM PIPES, 20mM NaCl, 2 M urea, pH 6.5, buffer, eluting with an increasing NaCl concentration (0.02 M to 1 M NaCl). Fractions containing collagen IX were pooled and dialyzed against 50 mM acetic acid and then concentrated.

SDS-PAGE analysis

SDS-PAGE was undertaken using 4-12% Bis-Tris gradient gels (Invitrogen) with the MES buffer system according to the manufacturer's instructions. Protein samples were diluted in loading buffer with a reducing reagent then heated to 95°C for 5 minutes. Silver staining of gel and peptide mass mapping of excised band were then performed.

Mass spectrometry

The identity of the recombinant protein was confirmed by electrospray ionisation (ESI) tandem mass spectrometry. Following SDS-PAGE the protein band thought to be the matrilin-3 A-domain was excised from the gel and subjected to in-gel digestion. In brief the sample was reduced with DTT, alkylated with iodoacetamide and digested with trypsin. The peptides produced were extracted from the gel with sequential washes of ammonium bicarbonate and 50% acetronitrile with the combined extract dried to approx 20 μl in a vacuum centrifuge. Mass spectrometry was performed on 5 μl of the sample using a Q-TOF Micro attached to a CapLC chromatography system (both Waters, UK). Proteins were separated by in-line reverse phase chromatography before analysis by tandem mass spectrometry. The results obtained were interrogated against the SWISSPROT database using ProteinLynx Global Server V1.1 searching software (Micromass UK Ltd).

The mass of the recombinant protein was analysed by mass spectrometry. Purified matrilin-3 A-domain was desalted using C4 reversed phase 'ZipTip' micro solid phase extraction tips (Millipore). The extracted samples were infused into an electrospray-time of flight mass spectrometer (LCT, Waters, UK) at a flow rate of 10 μl/min. The multiply charged spectra obtained were deconvoluted iteratively using maximum entropy software (Waters, UK) to produce a molecular weight for each species present.

Multiangle Laser Light Scattering (MALLS) analysis

Samples of purified recombinant protein were applied to a Superdex 75 gel filtration column (GE Healthcare) running at a flow rate of 0.5 ml/min with TBS buffer. Samples eluting from the column passed through an in-line DAWN EOS laser photometer (laser wavelength 682 nm) and an Optilab rEX refractometer with QELS dynamic light scattering attachment. Light scattering intensity and eluant refractive index (concentration) were analyzed using ASTRA v4.8 software to give a weight-averaged molecular mass (Mw). Following Superdex 75 chromatography, 0.5 ml fractions were collected and analyzed by SDS-PAGE and silver staining.

Circular Dichroism (CD)

Far UV (190-260 nm) CD spectra were recorded using a Jasco-810 spectro-polarimeter. Measurements were taken every 0.2 nm in a 0.05 cm path length cell. Spectra were corrected for buffer absorbance and represent an average of 10 scans. Spectra were recorded

in milli-degrees and converted to mean residue ellipticities using concentrations estimated by absorbance profiles at 280 nm. Estimation of secondary structure content was performed using CDSSTR software program.

Analytical Ultracentrifugation (AUC)

The sedimentation coefficient for matrilin-3 A-domain was determined from velocity experiments using the Optima XL-A ultracentrifuge (Beckman Instruments). The experiments were performed using double sector cells and a rotor speed of 48000 rpm, taking 150 scans at 1.5 minutes intervals at a wavelength of 230 nm and at a temperature of 20°C. The sedimenting boundaries were analysed using the program Sedfit v8.7 and the resulting apparent sedimentation coefficient ($s_{20,w}$) were corrected for standard conditions using the program Sednterp developed by Hayes, Laue and Philo (35). Hydrodynamic radius (R_H) and frictional ratio (f/f_o) which represents the deviation of the friction of the molecule from a theoretical sphere of the same molecular weight were also calculated using Sednterp.

Differential scanning calorimetry (DSC)

The proteins' denaturation temperatures were determined using differential scanning calorimetry (VP-DSC MicroCalorimeter, MicroCal Incorporated). The protein samples (0.15 mg/ml) were buffer exchanged using HiTrap Desalting columns (GE Healthcare) in 20 mM TrisHCl pH7.4, 150 mM NaCl or 20 mM TrisHCl pH7.4, 150 mM NaCl, 1 mM EDTA. Both buffers were used as reference solutions for the scans. Samples were scanned once for thermal unfolding from 15°C to 100°C. Data conversion and analysis were performed with Origin software (OriginLab Corporation, Northampton, MA).

Dual polarization Interferometry (DPI)

The DPI experiments were performed on a Farfield AnaLight instrument. Purified recombinant matrilin-3 A-domain (at a concentration of 200 μg/ml) was immobilized onto an amine functionalized AnaChip using BS^3 linker chemistry. Tris buffer (200 mM, pH7.4) was then added to block unreacted BS^3. After stabilizing the immobilized matrilin-3 A-domain with sufficient rinsing with Tris running buffer (20 mM Tris pH7.4, 50 mM NaCl), 10 mM EDTA was injected in order to chelate any metal ions present. The protein was then exposed to $ZnCl_2$ and $CaCl_2$ at increasing concentrations (10, 25, 50, 100, 300 and 1000 μM). Matrilin-3 A-domain was regenerated between the two different metal ions with 10 mM EDTA. A more detailed protocol has been described by Thompsett and colleagues (36).

Surface Plasmon Resonance Assay

The surface plasmon resonance assays were performed on a BIAcore 3000 instrument using a CM5 sensor chip (Biacore AB), and kinetic parameters were determined with the manufacturer's BIAevaluation 4.1 software. Purified recombinant matrilin-3 A-domain (at a concentration of 10 μg/ml) was immobilized at a flow rate of 12 μl/min for 12 minutes in sodium acetate pH 4.2 at 25°C onto different flow cells of the CM5 sensor chip. The chip surface was first activated by injection of 50 μl of a 1:1 mixture of 0.1 M *N*-hydroxysuccinimide and 0.4 M *N*-ethyl-N'-(dimethylaminopropyl)carbodiimide. Remaining active groups on the chip were blocked with 1 M ethanolamine-HCl pH 8.5. The immobilization resulted in 2500 resonance units for matrilin-3 A-domain. To study the effect of different cations on the binding properties of the matrilin-3 A-domain, type II collagen (10 μg/ml) was diluted in TBS buffer containing 1 mM of either Zn^{2+}, Ca^{2+}, Mg^{2+} or Mn^{2+} and was injected over the chip for 3 min at 20μl/min. To determine if the binding of the matrilin-3 A-domain was affected by the concentration of Zn^{2+} in the running buffer, we repeated the experiment with type II collagen using a range of Zn^{2+} concentrations from 0.025 mM to 1 mM. For all successive experiments, the running buffer was 20 mM TrisHCl

pH 7.4, 150 mM NaCl, 1 mM $ZnCl_2$, 0.005% (v/v) surfactant P20 (BIAcore). Kinetic runs were also performed using type II collagen (Sigma) and three different forms of type IX collagen as analytes. The analytes were injected for 6 min at 20 μl/min at concentrations ranging from 1-10 μg/ml (4-45 nM). The analytes were simultaneously passed over the control cell and this baseline was subtracted from the experimental flow cells. Tightly bound proteins were then dissociated by injection of 10 mM EDTA. To investigate the kinetics of interactions between matrilin-3 A-domain and cartilage oligomeric matrix protein (COMP), COMP (R&D) was immobilized on the surface of a CM5 sensor chip via amine coupling. By using 10 μg/ml of COMP, typically 4000 RU was immobilized, which was at a saturation level. Samples were applied to the sensor chip surface in 100 mM sodium acetate pH3.5. All subsequent binding experiments were performed in 20 mM TrisHCl pH 7.4, 150 mM NaCl, 1 mM $ZnCl_2$, 0.005% (v/v) surfactant P20 (BIAcore). Matrilin-3 A-domain was injected at concentrations ranging from 0 to 25 μg/ml (0-1100 nM) at a flow rate of 30 μl/min. Samples were injected for 5 min, dissociated for 10 min, regenerated for 1 min using 20 mM TrisHCl pH7.4, 1 M NaCl, and then stabilized for 20 min before the next injection. The analyte was simultaneously passed over a blank flow cell, and this baseline was subtracted from the experimental flow cell. None of the analytes was found to interact with the blank flow cell. After subtraction of each response value from the control cell, association and dissociation rate constants were determined by separate K_a/K_d fittings of the binding and dissociation curves using global data analysis. All curves were fitted using 1:1 Langmuir association/dissociation model (BIAevaluation 4.1. BIAcore AB).

Electron microscopy of the matrilin-3 A-domain, COMP and type IX collagen

Rotary shadowing transmission electron microscopy was performed as described previously (21). Briefly, a modified version of the mica sandwich technique was used to prepare 6 μl aliquots of each sample for platinum carbon rotary shadowing using the Cressington CFE-50B and Nickel 400 TEM grids. Replicas created by this method were studied using a JEOL 1200EX transmission electron microscope operated at an accelerating voltage of 100 kV. Electron micrographs were taken on Agfa Scientia 23D56 em film and then scanned onto a PC using a Polaroid Sprintscan 45 scanner, in preparation for image reproduction or digitized for analysis. Micrographs obtained were digitized from the photographic film using a monochrome TV camera (Bosch analogue type YK91D) for image analysis purposes. Matrilin-3 A-domain and COMP were mixed at a molar ratio of 1:1 and dialysed at 4°C against 20 mM Tris-HCl buffer (pH 7.4), containing 150 mM NaCl and 1 mM $ZnCl_2$.

RESULTS

Structure of recombinant matrilin-3 A-domain

Matrilin-3 A-domain was purified as a secreted protein and had an apparent molecular weight under denaturing conditions of ~22 kDa according to SDS-PAGE (Figure 1A). Tryptic peptide analysis by ESI tandem mass spectrometry validated the identity of the purified protein and ESI mass spectrometry revealed an expected intact mass for the purified protein of 22,031 Da (Supplemental 1). The purified protein was therefore confirmed to be the protein of interest and of the correct size. The ‘native’ protein was then analyzed by multi-angle light scattering coupled to gel filtration to yield a molecular weight of 24 kDa (Supplemental 2), which is consistent with a monomeric protein. Circular dichroism (CD) was used to determine the folding characteristics of the protein (Figure 1B). The average values for secondary structure composition following CDSSTR analysis were 15% α-helix, 27% β-sheet, 21% turn and 37 % random coil.

Conformational changes in the A-domain of matrilin-3 in the presence or absence of Zn^{2+}

In order to determine whether the conformation of the matrilin-3 A-domain was different in the presence or absence of Zn^{2+} we used sedimentation velocity experiments. In the presence of Zn^{2+}, the matrilin-3 A-domain sediments as a single species with a sedimentation coefficient of $2.4s_{20,w}$ and a R_H value of 2.38 nm (Figure 2A). There was no evidence of higher order oligomerization. The frictional ratio (f/f_o), which is a comparison of the friction of the molecule compared to a theoretical compact sphere, was 1.25 which suggests the protein is both compact and globular. However, when 2 mM EDTA was added to the sample the recombinant protein exhibited a lower sedimentation rate ($2.16s_{20,w}$) and an increase in R_H (2.65 nm) suggesting a less compact conformation (Figure 2A). A comparable difference in R_H was observed in the presence or absence of Zn^{2+} using a non-model based method (van Holde – Weischet), which corrects for the effects of diffusion and gave measurements of 2.42 nm and 2.76 nm respectively (data not shown). Sedimentation in the presence of Ca^{2+} revealed a similar profile to that found with EDTA (data not shown). Overall the sedimentation data confirm that in the presence of Zn^{2+} the matrilin-3 A-domain undergoes a conformational tightening.

To further elucidate the effect of divalent cations on the conformation of the A-domain, optical evanescent wave dual polarization interferometry (DPI) was used (37-39). This technique allowed us to measure in real time the structural changes occurring to the A-domain on the introduction of Zn^{2+} and Ca^{2+}. Increasing the concentrations of Zn^{2+} caused a subsequent increase in the differential refractive index (Figure 2B), which was associated with an increase in the density of the protein layer and a corresponding decrease (by 0.12 nm) in the thickness (Figure 2C). The protein effectively undertook a conformational change by becoming more compact in presence of Zn^{2+}. A k_d value of 7.5 mM was calculated for the affinity of Zn^{2+} binding to the matrilin-3 A-domain. These changes in density and thickness were not seen following the addition of Ca^{2+}, suggesting that Ca^{2+} does not promote this conformational change (data not shown).

Thermal stability of the matrilin-3 A-domain in the presence or absence of Zn^{2+}

In order to determine the thermal stability of the A-domain, differential scanning calorimetry (DSC) was used. Differences in heat uptake by the sample and reference cells (containing buffer only) were measured and the transition was fitted with a non-two-state model. The denaturation temperature of the matrilin-3 A-domain (in the presence of Zn^{2+}) was within the temperature range of 55-56°C and approximately 51°C in the presence of 2 mM EDTA (Figure 3), suggesting that the presence of Zn^{2+} stabilizes the A-domain. The thermal stability of the matrilin-3 A-domain was also assessed using CD by increasing the temperature linearly from 10 to 90°C and monitoring unfolding at 222 nm. A midpoint temperature of thermal denaturation of ~56°C was obtained, which was in agreement with the results obtained by DSC (data not shown).

Interactions between the matrilin-3 A-domain and collagen in the presence of different cations

It has previously been shown that full-length matrilin-3 can interact with type II and IX collagen *in vitro* (27). These data were confirmed by our own BIAcore studies, which produced k_d values of 5.9 nM and 1.5 nM respectively (Supplemental 3). We next wished to determine whether the matrilin-3 A-domain alone could support this binding and if there was a preference for different cations. Binding studies were therefore performed using four different cations (Zn^{2+}, Ca^{2+}, Mg^{2+} and Mn^{2+}) at a concentration of 1 mM each (Figure 4). These studies demonstrated that whilst 1 mM Zn^{2+} supported strong binding of type II and IX collagen to the matrilin-3 A-domain, in contrast, binding in the presence of 1 mM Ca^{2+}, Mg^{2+} or Mn^{2+} was negligible. We initially used a cation concentration of 1 mM because this

was consistent with previous studies performed by Budde *et al* on the binding of full-length matrilin-3 with type IX collagen (27). However, to determine if the matrilin-3 A-domain could bind to type II collagen in the presence of lower, and perhaps more physiologically relevant, concentrations of Zn^{2+}, we repeated these binding studies using a range of Zn^{2+} concentrations from 0.025 mM to 1 mM (Supplemental 4A). Overall, these data demonstrated that type II collagen could bind to the matrilin-3 A-domain over a broad range of Zn^{2+} concentrations. However, to maximize the binding response, all subsequent experiments were performed in the presence of 1 mM Zn^{2+}.

Binding of matrilin-3 A-domain to COMP and type II collagen

The kinetics of matrilin-3 A-domain binding to COMP and type II collagen was studied by surface plasmon resonance (Figure 5A). Our data establishes that COMP interacts with the matrilin-3 A-domain alone in the presence of 1 mM Zn^{2+} (Figure 5A) but not with 1 mM Ca^{2+} (data not shown). Kinetics of the interaction between the two proteins showed saturable binding and indicated an apparent k_d of 500 nM, χ^2=0.63 (n=3). Rotary shadowing TEM of purified matrilin-3 A-domain and COMP showed individual molecules when viewed separately (Figure 5B). The matrilin-3 A-domains were present as individual globular particles, whereas COMP had a characteristic bouquet structure with prominent C-terminal domains. Interestingly, when these molecules were incubated together in a 1:1 molar ratio prior to rotary shadowing, numerous filamentous structures were observed confirming the BIAcore studies and suggesting that the A-domain may act as a bridging molecule by bringing several COMP molecules together. Finally, we were also able to confirm that the A-domain of matrilin-3 was also able to bind with strong affinity (k_d of 6.27 nM) to type II collagen in the presence of 1 mM Zn^{2+} (Figure 5C), but not other cations (Figure 4). Moreover, the dissociation constant did not change significantly (k_d of 4.7 nM) when these experiments were repeated in the presence of 0.05 mM Zn^{2+} (Supplemental 4B).

Interactions between the matrilin-3 A-domain and different forms of type IX collagen

The interaction of matrilin-3 with the surface of cartilage fibrils occurs by direct interaction with type IX collagen (26,27). We therefore determined the binding affinity of the matrilin-3 A-domain for type IX collagen in the presence of Zn^{2+}. Kinetic analysis demonstrated that type IX collagen bound to the matrilin-3 A-domain in a dose-dependent manner (0-45 nM) and revealed an averaged k_d value of 1.37 nM with a χ^2 value of 0.94 for the curve fit (Figure 6A). The addition of 10 mM EDTA completely abolished the binding, confirming that the interaction between the matrilin-3 A-domain and type IX collagen was metal ion-dependent. Having established that the matrilin-3 A-domain bound specifically to full-length type IX collagen, we wished to identify the region(s) within type IX collagen that mediates this interaction. Binding studies with two different molecular forms of type IX collagen were therefore performed. These were the vitreous form of type IX collagen (i.e. lacking the NC4 domain) (40) (Figure 6B & D) and a mutated form which contained an in-frame deletion of 12 amino acid residues from the COL3 domain of the α3(IX) chain (Figure 6C & D). This mutation has previously been shown to result in MED (31) but does not appear to cause any overt disruption to the structure of the NC4/COL3 domain of type IX collagen as visualized by rotary shadowing TEM (Figure 6E). The matrilin-3 A-domain bound to the vitreous form of type IX collagen with a k_d value of 3.25 nM (χ^2= 0.96) (Figure 6B). However binding to type IX collagen was completely abolished when it contained the in-frame deletion (Figure 6C), suggesting that the matrilin-3 A-domain binds to type IX collagen through the COL3 domain.

DISCUSSION

In this study we have characterized the structure and interactions of the matrilin-3 A-domain. Recombinant matrilin-3 A-domain expressed by mammalian cell culture exists in a monomeric form with a mass of 22,031 Da and a thermal stability in the range of 55-56°C (in the presence of Zn^{2+}). Circular dichroism revealed a structure comprising 15% α-helix, 27% β-sheet, 21% turn, and 37 % random coil, which is very similar to that of the integrin I-domain, to which it has a high degree of sequence similarity (5). There are no previous reports describing conformational changes in the structure of A-domains, other than those described for integrins and the A-domain of complement factor B (22,24). However, it has been hypothesized that A-domains which contain a perfect MIDAS motif may also bind a metal ion and undergo an 'integrin switch' (24). In this study DPI analysis confirmed that Zn^{2+} binding to the matrilin-3 A-domain induces a tightening of the molecule, which is equivalent to an approximate 0.3 nm decrease in hydrodynamic radius when assayed by sedimentation analysis. These data therefore demonstrate that the matrilin-3 A-domain can bind to Zn^{2+} and undergo a conformational tightening similar to that previously described for the integrin I-domain (41,42) and the A-domain of Factor B (24,43). Human and mouse matrilin-3 have been reported to contain an 'imperfect' MIDAS motif (23,44) due to the perceived absence of threonine in loop 2, which is replaced by serine (i.e. TxTxS). However, a crystal structure of the A-domain of complement factor B predicts that the metal ion is coordinated by the first threonine residue of this loop (i.e. TxTxx) (24), suggesting that matrilin-3 might in fact have a 'perfect' MIDAS motif. Indeed, our findings support matrilin-3 having a perfect MIDAS motif. The conformational change was not observed with Ca^{2+}, suggesting that the matrilin-3 A-domain has acquired a requirement for specific metal-ions for activation and/or binding. It is possible that the conformational change induced by the presence of Zn^{2+} allows the matrilin-3 A-domain to interact with high affinity to other components of the ECM. Indeed, the activation of integrin I-domains through the binding of cations can dramatically alter affinity for their ligands.

It has previously been shown that recombinant full-length matrilin-3 interacts with recombinant type IX collagen (26,27). This binding is strongly dependent on the presence of divalent cations and the addition of EDTA effectively abolished binding (26,27). However, no studies have yet focused on the binding properties of the matrilin-3 A-domain alone. We therefore used BIAcore (surface plasmon resonance) to study the binding of type II and type IX collagen to the matrilin-3 A-domain in the presence of different cations. The A-domain of matrilin-3 bound with high affinity to type II and type IX collagen in the presence of Zn^{2+}. In both cases binding was abolished by the addition of EDTA confirming that this interaction was reversible and Zn^{2+}-dependent. Interestingly, the other cations (Ca^{2+}, Mg^{2+} and Mn^{2+}) did not support, to any great extent, the binding of type II and type IX collagen to matrilin-3 A-domain. A possible explanation of this finding is that the A-domain of matrilin-3 only possesses a biologically relevant conformation when it is bound to Zn^{2+}. One important factor that is relevant to these studies is the concentration of divalent cations at the site of interaction of these proteins *in vivo*. Different techniques have previously been used to measure the overall concentration of divalent cations in the cartilage ECM and these assays have produced concentrations of Zn^{2+} ranging from 0.16 mM to 1.85 mM and Ca^{2+} from 5 mM to 98 mM (25 and references therein). However, what is not known are the local differences in the concentration of divalent cations between the various layers of the articular cartilage or the different zones of the growth plate.

In order to determine where on type IX collagen the matrilin-3 A-domain was binding we performed BIAcore experiments with a truncated form of type IX collagen normally found in the vitreous of the eye (i.e. lacking the NC4 domain) (45). The NC4 domain is a compact non-collagenous globular domain and its location (projected away from the fibril body)

places it in an ideal position to facilitate interactions with other macromolecules of the cartilage extracellular matrix (19). Indeed, the NC4 domain of type IX collagen has been shown to interact with the C-terminal domain of COMP (20,21). It was therefore interesting to observe that there was still binding between the matrilin-3 A-domain and type IX collagen lacking the NC4 domain, suggesting that the NC4 domain is not required for this interaction to occur. In a further experiment we studied the interaction between the A-domain and a mutated form of type IX collagen, which contained an in-frame deletion of 12 amino acids (residues 50-61) from the COL3 domain of the α3(IX) chain. This deletion mutation has previously been shown to result in MED in unrelated patients (30-32). In this experiment binding was completely eliminated suggesting that the COL3 domain of type IX collagen mediates the interaction with the A-domain of matrilin-3. These data are in agreement with previous findings on the binding of full-length matrilin-3 to type IX collagen using solid phase assays (27). In these studies matrilin-3 interacted with full-length type IX collagen and type IX collagen in which the non-collagenous domains had been enzymatically removed from the molecule by pepsin digestion. Furthermore, binding was considerably reduced following the removal of the collagenous domains by digestion with collagenase (27). Our data are also consistent with binding studies performed between recombinant integrin I-domains and recombinant type IX collagen, which demonstrated that α_1I and α_2I bound to the COL3 domain of type IX collagen close to the NC3 domain (46). The COL3 domain has been described as an important functional domain of type IX collagen with a possible role in mediating interactions with other components of the cartilage ECM. Indeed, it has been reported that recombinant matrilin-3 A-domain (expressed in E. *Coli*) bound to the individual chains of the COL3 domain of type IX collagen and with highest apparent affinity for α3(IX) COL3 (47). In this study we have demonstrated the detrimental effect of an MED-causing deletion in the COL3 domain on the binding of type IX collagen to the matrilin-3 A-domain. We therefore hypothesize that the COL3 domain of type IX collagen plays an important role in the pathophysiology of MED and that these observations might best explain why MED mutations in type IX collagen cluster in a restricted region within the COL3 domain.

Finally, the role of Zn^{2+} in the formation of the matrilin-3 A-domain/collagen complexes is yet to be fully defined and this includes the identity of the metal-coordinating residue(s) in the type II and type IX collagen molecules. It has previously been determined that binding between the I-domain of integrin α2β1 and a triple helical collagen peptide is mediated through a GFOGER motif, in which the glutamate residue completes the coordination of the metal ion (41). Our studies have shown that the matrilin-3 A-domain binds to the COL3 domain of type IX collagen and that this binding is abolished by the in-frame deletion of 12 amino acids (residues 50-61: GEAGPPGLPGPP) from the COL3 domain of the α3(IX) chain. It is therefore interesting to note that this region of α3(IX)-COL3 contains a glutamate residue, and its deletion in the MED mutant form may be impacting on the binding between matrilin-3 and type IX collagen. However, it is entirely possible that type IX collagen has a matrilin-3 binding site that extends over all three chains, which could explain the grouping of MED mutations to the equivalent regions of the COL3 domain (10). Heterotrimeric type IX collagen also contains histidine (21 residues) and cysteine (20 residues), which are capable of coordinating metal ion binding, however the COL3 domain of type IX collagen does not contain any of these particular residues.

In summary, therefore, we have described the structure of the matrilin-3 A-domain in solution and the conformational changes induced by the presence or absence of Zn^{2+}. These data imply a critical structural role for this domain and highlights the importance of the tight conformation for its binding to other ECM proteins. In these studies we have also identified the precise domain in collagen type IX that mediates the interaction with matrilin-3 A-domain. Matrilin-3 A-domain appears to bind exclusively through the COL3 domain of type

IX collagen. Disruptions to these interactions through mutation are therefore likely to play a role in the development of human skeletal dysplasia and therefore further biochemical/biophysical characterization of the COMP-matrilin-collagen IX network may provide novel insight into disease mechanisms in the MED bone dysplasia family.

Supplementary Material

Refer to Web version on PubMed Central for supplementary material.

Acknowledgments

This work was supported by a grant from the Wellcome Trust (Michael Briggs is the recipient of a Wellcome Trust Senior Research Fellowship in Basic Biomedical Science; Grant 071161/Z/03/Z) and the work was undertaken in the Wellcome Trust Centre for Cell-Matrix Research and the Biomolecular Analysis Core Facility in the Faculty of Life Sciences at the University of Manchester. We would like to thank Marcus Swann (Farfield Scientific Ltd.) for his help with DPI data analysis. We are also grateful to Dr David Knight for the mass spectrometry and Marj Howard for technical help with the light scattering.

REFERENCES

1. Klatt AR, Nitsche DP, Kobbe B, Morgelin M, Paulsson M, Wagener R. J Biol Chem. 2000; 275(6): 3999–4006. [PubMed: 10660556]
2. Wagener R, Ehlen HW, Ko YP, Kobbe B, Mann HH, Sengle G, Paulsson M. FEBS Lett. 2005; 579(15):3323–3329. [PubMed: 15943978]
3. Belluoccio D, Schenker T, Baici A, Trueb B. Genomics. 1998; 53(3):391–394. [PubMed: 9799608]
4. Wagener R, Kobbe B, Paulsson M. FEBS Lett. 1997; 413(1):129–134. [PubMed: 9287130]
5. Chapman KL, Mortier GR, Chapman K, Loughlin J, Grant ME, Briggs MD. Nat Genet. 2001; 28(4): 393–396. [PubMed: 11479597]
6. Jackson GC, Barker FS, Jakkula E, Czarny-Ratajczak M, Makitie O, Cole WG, Wright MJ, Smithson SF, Suri M, Rogala P, Mortier GR, Baldock C, Wallace A, Elles R, Ala-Kokko L, Briggs MD. J Med Genet. 2004; 41(1):52–59. [PubMed: 14729835]
7. Cotterill SL, Jackson GC, Leighton MP, Wagener R, Makitie O, Cole WG, Briggs MD. Hum Mutat. 2005; 26(6):557–565. [PubMed: 16287128]
8. Leighton MP, Nundlall S, Starborg T, Meadows RS, Suleman F, Knowles L, Wagener R, Thornton DJ, Kadler KE, Boot-Handford RP, Briggs MD. Hum Mol Genet. 2007
9. Otten C, Wagener R, Paulsson M, Zaucke F. J Med Genet. 2005; 42(10):774–779. [PubMed: 16199550]
10. Briggs MD, Chapman KL. Hum Mutat. 2002; 19(5):465–478. [PubMed: 11968079]
11. Oldberg A, Antonsson P, Lindblom K, Heinegard D. J Biol Chem. 1992; 267(31):22346–22350. [PubMed: 1429587]
12. Hedbom E, Antonsson P, Hjerpe A, Aeschlimann D, Paulsson M, Rosa-Pimentel E, Sommarin Y, Wendel M, Oldberg A, Heinegard D. J Biol Chem. 1992; 267(9):6132–6136. [PubMed: 1556121]
13. DiCesare P, Hauser N, Lehman D, Pasumarti S, Paulsson M. FEBS Lett. 1994; 354(2):237–240. [PubMed: 7957930]
14. Shen Z, Heinegard D, Sommarin Y. Matrix Biol. 1995; 14(9):773–781. [PubMed: 8785592]
15. Smith RK, Zunino L, Webbon PM, Heinegard D. Matrix Biol. 1997; 16(5):255–271. [PubMed: 9501326]
16. Newton G, Weremowicz S, Morton CC, Copeland NG, Gilbert DJ, Jenkins NA, Lawler J. Genomics. 1994; 24(3):435–439. [PubMed: 7713493]
17. Kennedy J, Jackson G, Ramsden S, Taylor J, Newman W, Wright MJ, Donnai D, Elles R, Briggs MD. Eur J Hum Genet. 2005; 13(5):547–555. [PubMed: 15756302]
18. Kennedy J, Jackson GC, Barker FS, Nundlall S, Bella J, Wright MJ, Mortier GR, Neas K, Thompson E, Elles R, Briggs MD. Hum Mutat. 2005; 25(6):593–594. [PubMed: 15880723]
19. Olsen BR. Int J Biochem Cell Biol. 1997; 29(4):555–558. [PubMed: 9363632]

20. Thur J, Rosenberg K, Nitsche DP, Pihlajamaa T, Ala-Kokko L, Heinegard D, Paulsson M, Maurer P. J Biol Chem. 2001; 276(9):6083–6092. [PubMed: 11084047]
21. Holden P, Meadows RS, Chapman KL, Grant ME, Kadler KE, Briggs MD. J Biol Chem. 2001; 276(8):6046–6055. [PubMed: 11087755]
22. Takagi J, Springer TA. Immunol Rev. 2002; 186:141–163. [PubMed: 12234369]
23. Whittaker CA, Hynes RO. Mol Biol Cell. 2002; 13(10):3369–3387. [PubMed: 12388743]
24. Bhattacharya AA, Lupher ML Jr. Staunton DE, Liddington RC. Structure. 2004; 12(3):371–378. [PubMed: 15016353]
25. Rosenberg K, Olsson H, Morgelin M, Heinegard D. J Biol Chem. 1998; 273(32):20397–20403. [PubMed: 9685393]
26. Mann HH, Ozbek S, Engel J, Paulsson M, Wagener R. J Biol Chem. 2004; 279(24):25294–25298. [PubMed: 15075323]
27. Budde B, Blumbach K, Ylostalo J, Zaucke F, Ehlen HW, Wagener R, Ala-Kokko L, Paulsson M, Bruckner P, Grassel S. Mol Cell Biol. 2005; 25(23):10465–10478. [PubMed: 16287859]
28. Nicolae C, Ko YP, Miosge N, Niehoff A, Studer D, Enggist L, Hunziker EB, Paulsson M, Wagener R, Aszodi A. J Biol Chem. 2007
29. Chen Q, Zhang Y, Johnson DM, Goetinck PF. Mol Biol Cell. 1999; 10(7):2149–2162. [PubMed: 10397755]
30. Bonnemann CG, Cox GF, Shapiro F, Wu JJ, Feener CA, Thompson TG, Anthony DC, Eyre DR, Darras BT, Kunkel LM. Proc Natl Acad Sci U S A. 2000; 97(3):1212–1217. [PubMed: 10655510]
31. Paassilta P, Lohiniva J, Annunen S, Bonaventure J, Le Merrer M, Pai L, Ala-Kokko L. Am J Hum Genet. 1999; 64(4):1036–1044. [PubMed: 10090888]
32. Lohiniva J, Paassilta P, Seppanen U, Vierimaa O, Kivirikko S, Ala-Kokko L. Am J Med Genet. 2000; 90(3):216–222. [PubMed: 10678658]
33. Pihlajamaa T, Perala M, Vuoristo MM, Nokelainen M, Bodo M, Schulthess T, Vuorio E, Timpl R, Engel J, Ala-Kokko L. J Biol Chem. 1999; 274(32):22464–22468. [PubMed: 10428821]
34. Nokelainen M, Helaakoski T, Myllyharju J, Notbohm H, Pihlajaniemi T, Fietzek PP, Kivirikko KI. Matrix Biol. 1998; 16(6):329–338. [PubMed: 9503366]
35. Lebowitz J, Lewis MS, Schuck P. Protein Sci. 2002; 11(9):2067–2079. [PubMed: 12192063]
36. Thompsett AR, Brown DR. Biochim Biophys Acta. 2007; 1774(7):920–927. [PubMed: 17573247]
37. Karim K, Taylor JD, Cullen DC, Swann MJ, Freeman NJ. Anal Chem. 2007; 79(8):3023–3031. [PubMed: 17367112]
38. Ricard-Blum S, Peel LL, Ruggiero F, Freeman NJ. Anal Biochem. 2006; 352(2):252–259. [PubMed: 16545768]
39. Swann MJ, Peel LL, Carrington S, Freeman NJ. Anal Biochem. 2004; 329(2):190–198. [PubMed: 15158477]
40. Nishimura I, Muragaki Y, Olsen BR. J Biol Chem. 1989; 264(33):20033–20041. [PubMed: 2584206]
41. Emsley J, Knight CG, Farndale RW, Barnes MJ, Liddington RC. Cell. 2000; 101(1):47–56. [PubMed: 10778855]
42. Lee JO, Bankston LA, Arnaout MA, Liddington RC. Structure. 1995; 3(12):1333–1340. [PubMed: 8747460]
43. Hinshelwood J, Perkins SJ. J Mol Biol. 2000; 298(1):135–147. [PubMed: 10756110]
44. Ko YP, Kobbe B, Paulsson M, Wagener R. Biochem J. 2005; 386(Pt 2):367–379. [PubMed: 15588228]
45. Bishop PN, Crossman MV, McLeod D, Ayad S. Biochem J. 1994; 299(Pt 2):497–505. [PubMed: 8172611]
46. Kapyla J, Jaalinoja J, Tulla M, Ylostalo J, Nissinen L, Viitasalo T, Vehvilainen P, Marjomaki V, Nykvist P, Saamanen AM, Farndale RW, Birk DE, Ala-Kokko L, Heino J. J Biol Chem. 2004; 279(49):51677–51687. [PubMed: 15383545]
47. Wu, J.; Hanson, D.; Eyre, D. University of Washington Department of Orthopaedics and Sports Medicine 2004 Report. 2004.

48. Schuck P, Perugini MA, Gonzales NR, Howlett GJ, Schubert D. Biophys J. 2002; 82(2):1096–1111. [PubMed: 11806949]

Europe PMC Funders Author Manuscripts

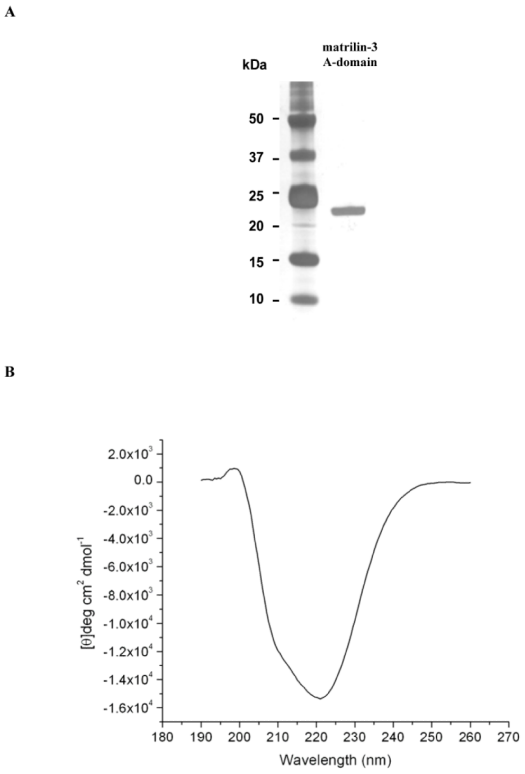

Fig. 1. Purification and characterization of recombinant matrilin-3 A-domain

(*A*) Silver stained SDS-PAGE gel of purified recombinant matrilin-3 A-domain under reducing conditions; Lane 1 is molecular weight marker and lane 2 is the purified recombinant matrilin-3 A-domain, which is resolved as a single band of ~22 kDa. (*B*) Circular dichroism (CD) spectrum of recombinant matrilin-3 A-domain. The CD spectrum of the purified matrilin-3 A-domain was monitored between 190 and 260 nm in 20 mM Tris buffer, 150 mM NaCl pH 7.4 at 25 °C. These data reveal that the purified protein is folded with characteristic β-sheet and α-helical elements within the secondary structure.

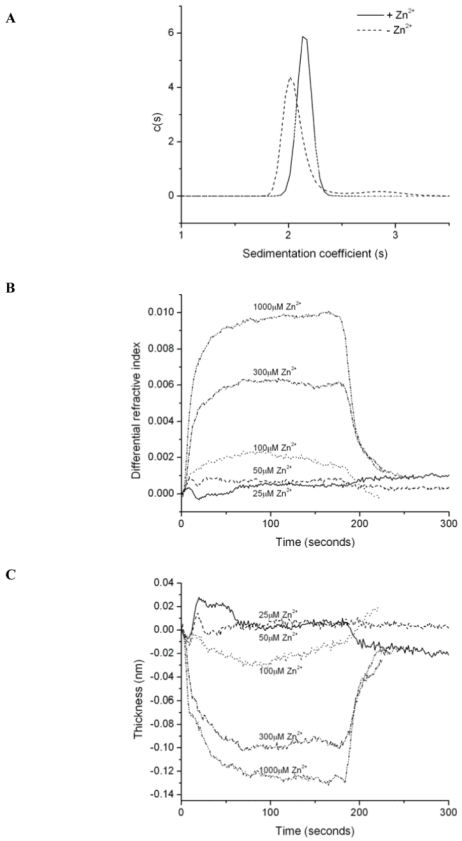

Fig. 2. Structural analysis of recombinant matrilin-3 A-domain in the presence or absence of Zn^{2+}

(*A*) Sedimentation velocity of recombinant matrilin-3 A-domain in presence or absence of Zn^{2+} analyzed by the distribution of Lamn equation solutions c(s) model using the program Sedfit (48). In the presence of Zn^{2+} (▬) the protein sediments as a single species with a sedimentation coefficient of 2.4s. In absence of Zn^{2+} (----) the protein become less compact, which is reflected in a smaller sedimentation coefficient (2.16s). (*B* & *C*) Dual polarization Interferometry (DPI) monitoring real time density (refractive index) and dimension profiles of matrilin-3 A-domain indicating structural changes upon exposure to Zn^{2+}. (*B*) Density change as a function of an increasing concentration of Zn^{2+} ranging from 25 to 1000 μM. (*C*) Changes in the thickness of the layer as a function of Zn^{2+} injections ranging from 25 to 1000 μM.

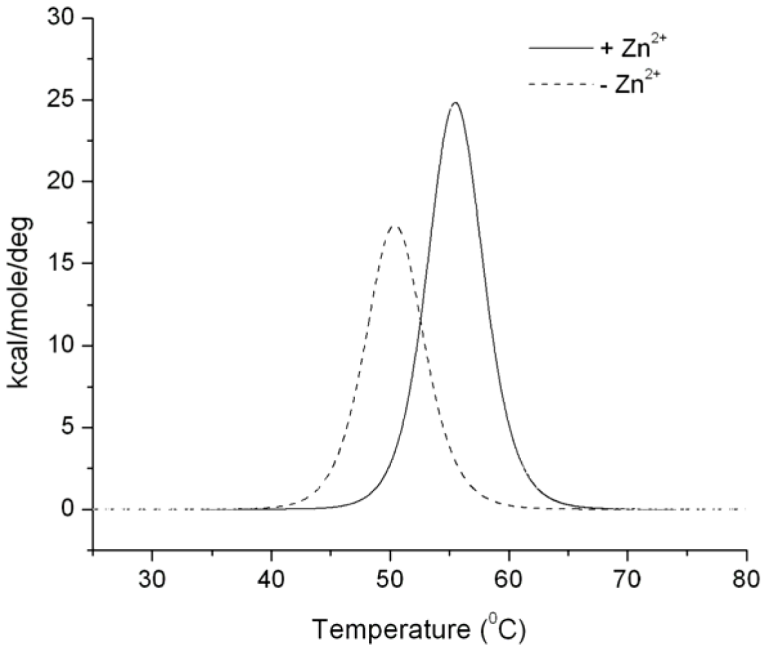

Fig. 3. Thermal stability of the recombinant matrilin-3 A-domain

The denaturation heat capacity curves were measured by differential scanning microcalorimetry (DSC) in the presence or absence of Zn^{2+}. The DSC profiles for recombinant matrilin-3 A-domain indicate a more stable conformation in the presence of Zn^{2+} (▬) with a T_m of 56°C as opposed to 51°C after removal of Zn^{2+}(----).

Europe PMC Funders Author Manuscripts

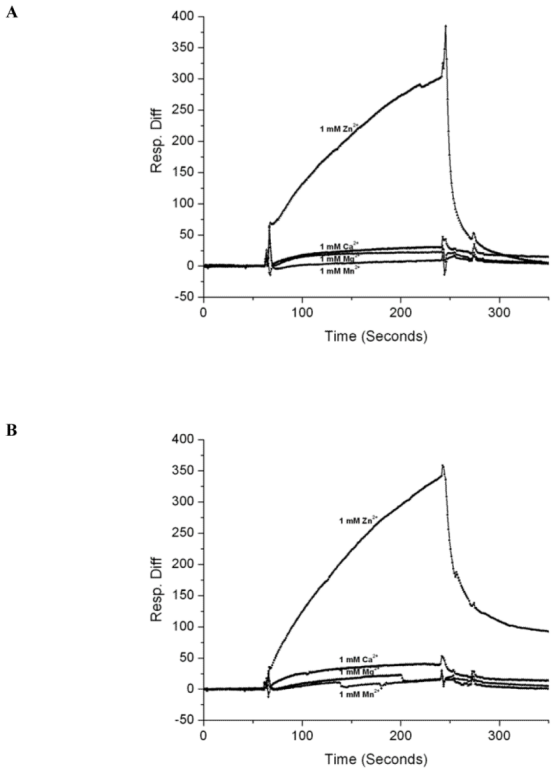

Fig. 4. The effect of four different cations (Zn^{2+}, Ca^{2+}, Mg^{2+} and Mn^{2+}) on the binding of type II and IX collagen to the matrilin-3 A-domain

(*A*) Binding of type II collagen (10 μg/ml) to the matrilin-3 A-domain in the presence of 1 mM Zn^{2+}, Ca^{2+}, Mg^{2+} or Mn^{2+}. (*B*) Binding of type IX collagen (10 μg/ml) to the matrilin-3 A-domain in the presence of 1 mM Zn^{2+}, Ca^{2+}, Mg^{2+} and Mn^{2+}.

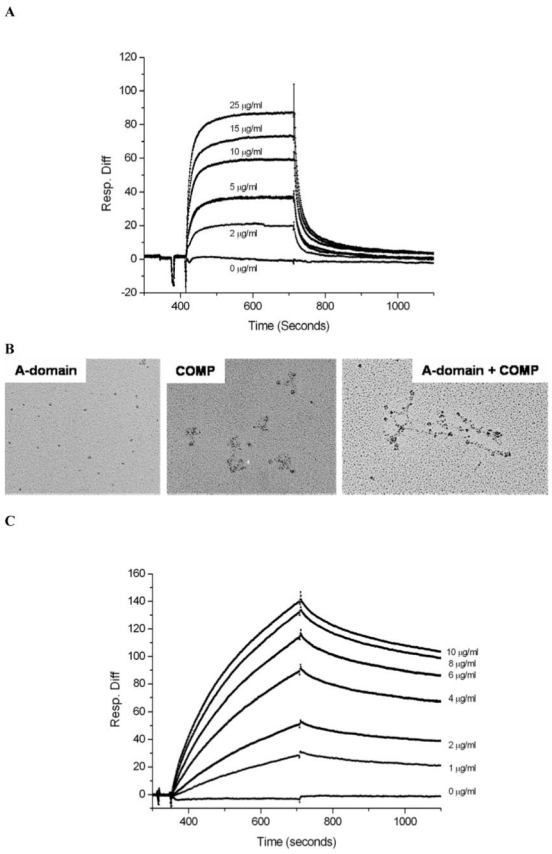

Fig. 5. Interactions of the matrilin-3 A-domain with COMP and type II collagen

(*A*) Binding to COMP. Matrilin-3 A-domain was injected over immobilized recombinant COMP at different concentrations ranging from 0 to 25 μg/ml. (*B*) Representative images of matrilin-3 A-domain, COMP and A-domain + COMP as observed by rotary shadowing TEM (images not to scale). (*C*) Binding to collagen type II. Full length type II collagen was injected over immobilized matrilin-3 A-domain at concentrations ranging from 0 to 10 μg/ml.

Europe PMC Funders Author Manuscripts

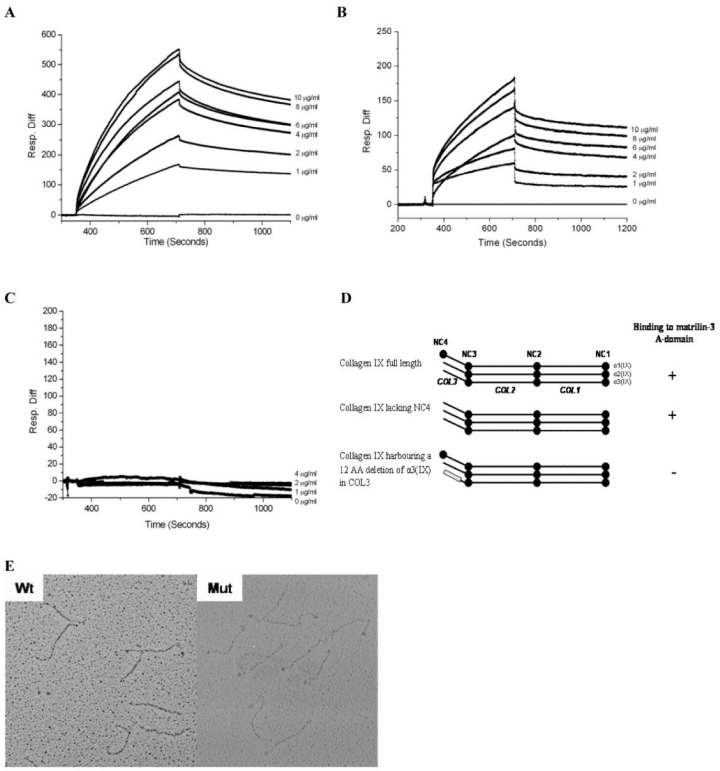

Fig. 6. Interactions of the matrilin-3 A-domain and type IX collagen

(*A*) Binding of matrilin-3 A-domain to full length type IX collagen. Full length type IX collagen was injected at concentrations ranging from 0 to 10 μg/ml. (*B*) Binding of matrilin-3 A-domain to type IX collagen lacking the NC4 domain (vitreous form). The truncated collagen IX was injected at concentrations ranging from 0 to 10 μg/ml. (*C*) Binding of matrilin-3 A-domain to type IX collagen harbouring a 12 amino acid deletion in the COL3 domain α3(IX) chain (MED form). The mutated form of type IX collagen was injected at concentrations ranging from 0 to 10 μg/ml. (*D*) Cartoon representations of the three type IX collagen variants and a summary of binding to the matrilin-3 A-domain. (*E*) Rotary shadowing TEM of full-length wild type (left panel) and mutant (right panel) type IX collagen.

Europe PMC Funders Author Manuscripts